Z. Phys. C – Particles and Fields 33, 465–473 (1987)

Zeitschrift für Physik C Particles and Fields
© Springer-Verlag 1987

Study of High $p_\perp$ Quark and Gluon Jet Fragmentation

P. Ghez[1] and G. Ingelman[2]

[1] L.A.P.P., BP 909, F-74019 Annecy-le-Vieux Cedex, France

[2] Deutsches Elektronen-Synchrotron DESY, Notkestrasse 85, D-2000 Hamburg 52, Federal Republic of Germany

Received 20 October 1986

Abstract. The fragmentation properties of high-$p_\perp$ jets are investigated using new data from the ISR and the SPS collider. Effects from gluon radiation are clearly demonstrated by comparison with a state-of-the-art model inlcuding QCD parton cascade evolution and string hadronization, which gives in general good agreement with the data. Differences between quark and gluon jets are discussed as well as Q^2-dependent scaling violation effects.

1. Introduction

In spite of the success of perturbative QCD to describe many experimental observations, like jet production properties [1], we still lack a basic understanding of the jet fragmentation process. In fact, the confinement induced transition from pertubatively produced partons to experimentally observable hadrons is one of the major unsolved problems in high energy physics. Nevertheless, phenomenologically successfull models have been developed to describe the observations and systematize our experiences from different kinds of interactions. To the extent that these models are not just parametrizations of data, but rather based on more or less elaborate physical models, they can have a large predictive power leading to useful tests of the underlying assumptions of the models.

The last few years have seen significant improvement on the perturbative description of jet evolution. The dynamics of the parton branching processes leading to a cascade of partons can thus be simulated by Monte Carlo methods and the subseqeunt non-perturbative hadronization be modelled to obtain a complete description of the jet. These models must, of course, be confronted with experimental observations and the recent results [2–4] on high-$p_\perp$ jets produced at CERN in high energy hadronic collisions are here of primary interest. In this paper we perform such a comparison with a particular model [5, 6] which represents the present understanding of jet fragmentation. In Sect. 2, the model is discussed in some detail and in Sect. 3 the data sample is described. Section 4 contains the actual comparison and we end with a more general discussion in Sect. 5.

2. The Model

There are several Monte Carlo implementations [5, 7–11] to simulate high-$p_\perp$ jet phenomena in hadron-hadron scattering. Their basic ingredients are similar although they differ in details of both the perturbative and non-perturbative parts (for a review see [12]). For the detailed calculations we use the Lund program [5, 6]. Other models should give essentially the same overall results although they will differ in details.

The starting point is the hard parton scattering cross-section in QCD,

$$d\sigma = \sum_{i,j,k} f_i(x_1, Q^2) \cdot f_j(x_2, Q^2) \cdot \frac{d\hat{\sigma}_{ijk}}{d\hat{t}}\, dx_1\, dx_2\, d\hat{t} \qquad (1)$$

including all leading order $(\alpha_s^2)\, 2 \to 2$ parton level processes. We use the structure function parametrizations of [13], but note that this choice is of little importance for the fragmentation properties. The two partons emerging from the hard scattering can be off mass shell, up to $O(Q)$, and are therefore expected to emit bremsstrahlung gluons to produce a shower of partons as illustrated in Fig. 1. The details of such a parton cascade evolution has been examined by several authors [14, 15] with the common feature of using the Altarelli-Parisi splitting functions for each separate branching. This is justified by the factorization of the cascade cross-section into the product of the probabilities for each separate branching provided

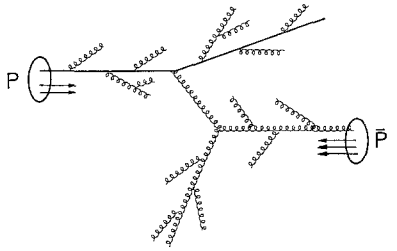

Fig. 1. Schematic illustration of high-$p_\perp$ scattering with initial and final state parton radiation

that the (offshell) parton masses are strongly reduced in each branching. This result in an iterative process, suitable for Monte Carlo simulation, which is stopped when the parton masses are below a chosen cut off value, $\sqrt{t_{\text{cut}}}$. Together with Λ_{QCD} this cut off regulates the amount of bremsstrahlung emitted. Interference effects between soft gluons are taken into account by the angular ordering method of [15].

The perturbative approximation become less reliable and eventually breaks down when the virtual parton masses become small. This is due to the increase of α_s with the decrease of the momentum transfer which is related to the virtuality, m^2, of the parent parton in a particular branching. The parameter t_{cut} determines the border line between the perturbative and non-perturbative regions of QCD. Unfortunately, there is no theoretical motivation for the choice of a particular t_{cut} value. It is rather related to ones confidence in the perturbative QCD cascade approach as well as the method used for hadronizing the resulting parton state. A complete model which includes the soft hadronization should, however, have as little dependence as possible on the exact value chosen for this parameter. This is discussed in [16] for a few alternative hadronization models.

In the Lund approach [17], which is used here, a colour triplet string connects all partons according to their colour ordering which is known from the perturbative cascade. Thus, the string can have a rather complicated topology, e.g. being stretched from a quark via several gluons before ending up on an antiquark. This requires the improvements of the model developed in [18] to handle short string segments between nearby partons. As shown in [16, 19], the string model provides the required stability with respect to t_{cut} changes.

Parton cascade evolution also occurs as a result of gluon radiation from the incoming partons before they make the hard scattering, Fig. 1. This is included according to the 'backwards' evolution scheme of [20]. For the fragmentation properties of the high-$p_\perp$ jets studied here, this is of less importance and will not be discussed in detail. The string treatment of beam-jets is also of less importance, although both of these issues will influence the low-$p_\perp$ background under the high-$p_\perp$ jets and thereby the soft part of the jet. Since most jet properties investigated in this study are dominated by the more energetic particles this is usually not a problem, but when soft particles do play a role we take special precautions as discussed below.

3. The Data Sample

The data from the UA1 collaboration [4] used for this study is based on the 1983 run at $\sqrt{s}=546$ GeV with an integrated luminosity of 118 nb^{-1}. Details of the trigger and selection criteria are given in [4, 21]. In short, the events were obtained by a hardware trigger on central jets with $E_\perp$ larger than a threshold varying between 15 and 25 GeV. To avoid trigger bias effects, essentially only away jets, i.e. jets opposite to the trigger jet, were used in the analysis giving 10,007 jets satisfying:

$$|\eta_{\text{jet}}|<1.4 \text{ or } 1.7<|\eta_{\text{jet}}|<2.5$$
$$p_{\perp\text{jet}}>15 \text{ GeV (with } \langle p_{\perp\text{jet}}\rangle=39 \text{ GeV)}.$$

This sample corresponds to a clean two-jet topology where events having a third jet with $p_{\perp 3}>0.2 \times \frac{p_{\perp 1}+p_{\perp 2}}{2}$ or $|\cos\theta_3^*|<0.8$ were removed (θ_3^* is the angle of the third jet with respect to the beam in the parton-parton c.m.s.). The removal of three-jet events has only a small influence on the longitudinal fragmentation properties, but significantly affects the transverse properties as discussed below.

The energy and direction of a jet as obtained from the calorimeter measurement and jet finding algorithm are corrected for experimental inefficiences using a method based on jet simulation with ISAJET [7] combined with detector simulation [21]. The 'true' jet momentum was thereby considered to be given by the parton from the hard scattering before final state radiation and hadronization. This can be noticably different from, e.g., defining the jet momentum from all hadrons inside a particular cone. We also note that, in ISAJET, a gluon is fragmented as a quark of random flavour and therefore the only difference between a quark- and gluon-initiated jet lies in the perturbative cascade. This may underestimate the difference of quark and gluon jets. However, the energy corrections applied to the data are global, i.e. flavour independent.

A charged particle is assigned to a jet if its track is close enough to the jet axis as measured in the

space of pseudorapidity and azimuthal angle, i.e.

$$\Delta R = \sqrt{(\eta_{\text{jet}} - \eta_{\text{track}})^2 + (\phi_{\text{jet}} - \phi_{\text{track}})^2} \leqq 1, \quad (2)$$

and its fractional jet momentum not too small

$$z = \frac{\bar{p}_{\text{track}} \cdot \bar{p}_{\text{jet}}}{|\bar{p}_{\text{jet}}|^2} \geqq 0.01. \quad (3)$$

The model events were obtained by the Monte Carlo program of [5, 6] and criteria applied so as to resemble the experimental situation. Jet events were defined by a minimum transverse momentum of 33 GeV in the hard scattering and, due to the mentioned correction procedure, jet momenta defined by the offshell parton emerging from this $2 \to 2$ process. Only jets within the experimental region of acceptance were used although essentially the same results are found if all jets are included in the analysis. Hence, the effects due to limitations in the experimental acceptance is generally small. With the effects from the initial state bremsstrahlung, the $p_\perp$ distribution of jets is in reasonable agreement with the experimental one, although the latter has a longer tail to smaller $p_\perp$ due to the trigger and efficiency properties. The kinematics of the two-jet system, like momentum transfer Q^2 and invariant mass M_{jj} of the two-jet system, also show good agreement. The subprocesses occuring in the selected event sample are 19% $qq \to qq$, 46% $qg \to qg$ and 35% $gg \to gg$ (q is here a quark or antiquark of any flavour). Gluon jets, which globally make up 58% of the jet sample, dominate for central rapidities, $|\eta| < 1$, and in the low transverse energy region, $E_\perp < 70$ GeV.

4. Results

4.1 Inclusive Jet Properties

We first consider the inclusive fragmentation function

$$D(z) = \frac{1}{N_{\text{jet}}} \cdot \frac{dN_{\text{ch}}}{dz} \quad (4)$$

for charged particles with z defined as in (3). Figure 2 shows the UA1 data [4] and for comparison also ISR data from the AFS collaboration [3]. The reason for the collider jets to be considerably softer is twofold. Firstly, they are dominated by gluon jets, $\approx 60\%$ according to the model, whereas the ISR jet sample contains $\approx 70\%$ quark jets. Secondly, the harder interaction at the collider, resulting in $\langle p_{\perp \text{jet}} \rangle \approx 39$ GeV compared to 13 GeV at the ISR, leads to stronger scaling violations; an effect which is also more accentuated for the colour octet source of a gluon jet. These effects are also borne out in the Monte Carlo calcula-

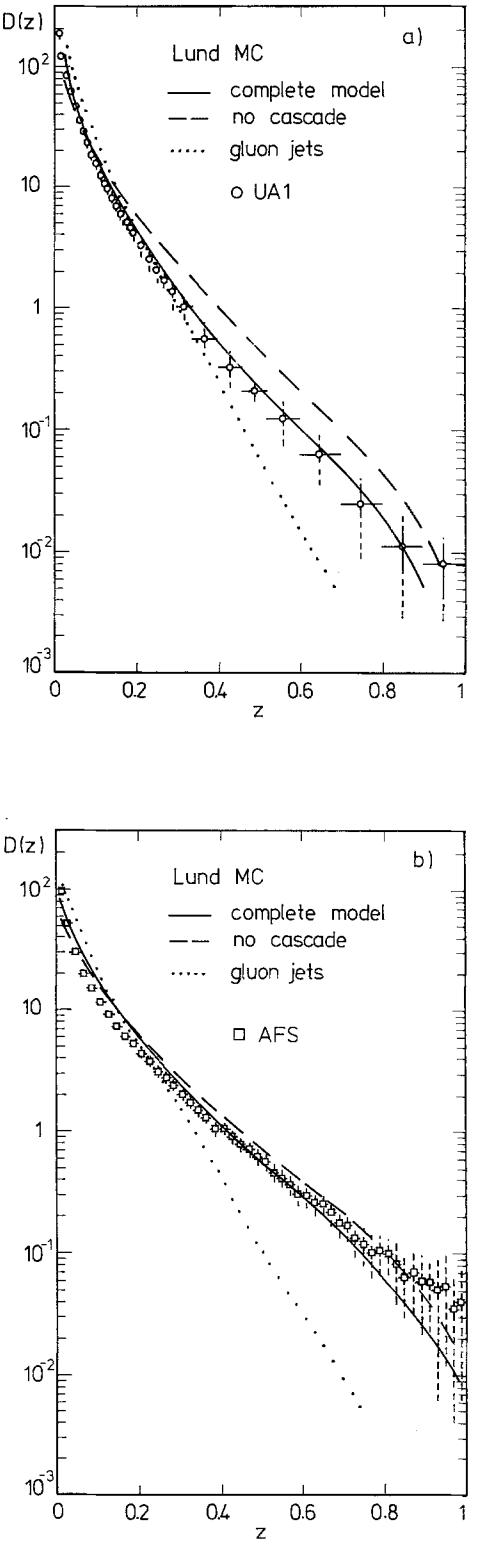

Fig. 2a, b. Fragmentation functions, (4), of high-$p_\perp$ jets at SPS collider **a** and ISR **b** energies. Data from UA1 [4] and AFS [3] collaborations with statistical (full) and systematic (dashed) error bars. The curves represent the model with the parton cascade included (full) and excluded (dashed), with quark and gluon jets mixed according to their relative cross-sections. Pure gluon jets including cascade are also shown (dotted curve) for comparison

tions. A few comments on model parameters are, however, needed at this point.

Based on the assumption of universality of the non-perturbative hadronization process, the parameters of the string fragmentation model was kept at their values obtained from comparisons with data from e^+e^- annihilation and deep inelastic scattering. In this approach therefore, only the parameters of the parton cascade evolution can be modified. For $\Lambda_{\rm QCD}$ we use 250 MeV after having verified that reasonable variations do not give significant changes of the examined observables. The parton shower cut off can be chosen in the range $2<\sqrt{t_{\rm cut}}<4$ GeV to obtain equally good agreement with the UA1 data (both for $D(z)$ and the following $p_\perp$ spectra). A lower value, like 1 GeV, can in fact also be accomodated together with a change of the fragmentation parameters still in agreement with e^+e^- data. The large-z region of the AFS data, although having large systematic errors as indicated, favours a larger value and hence we use $\sqrt{t_{\rm cut}}=4$ GeV. Still, the limit as $z\to 1$ is not well reproduced by the model which has a behaviour $D(z)\to 0$ not observed in the data. This may indicate an inadequacy of the fragmentation model, but we note that the $z\to 1$ limit of the collider data is well reproduced as is also the case with e^+e^- data [22] and that the systematic errors in this z-region are usually dominated by the jet energy determination. For very low z, where the underlying event contributes, the model simulation is not expected to be perfect because of the lack of understanding of the beam jets. Nevertheless, the model reproduces both ISR and $Sp\bar{p}S$ data quite well over essentially the whole z-range.

Whereas the importance of the QCD parton bremsstrahlung process for collider jets is clearly demonstrated by comparing the model result without it, dashed curve in Fig. 2a, its effect on ISR jets is rather small. An important feature of the model is the considerably softer spectrum of gluon jets as compared to quark jets, illustrated by the dotted lines in Fig. 2 which represent pure gluon Monte Carlo samples. This, together with the difference in scaling violations, accounts for the significantly softer gluon dominated collider jet sample compared to the quark dominated ISR jet sample. It is worth noting, however, that in spite of the dominance of gluon jets in the global collider jet sample, quark jets give the dominant contribution in the large z region due to their harder fragmentation function, see Fig. 2a. In this region therefore, the difference between ISR and collider jets are mainly due to scaling violation effects at the different Q^2 scales.

Another aspect of the longitudinal fragmentation of a jet is shown by the rapidity distribution of particles along the jet axis, Fig. 3, which reveals the expected rapidity plateau. The model without cascade gives a significantly lower plateau and a corresponding longer tail to large rapidities whereas the complete model gives a good description of the data. We note that the large rapidity tail, which corresponds to small angles ($y=4$ and 5 correspond approximately to 2 and 1 degree respectively), is sensitive to the precise jet axis definition. By extrapolation of the rapidity plateau to $y=0$ as in [4] a jet multiplicity can be defined by integrating the distribution. In Fig. 4 this multiplicity is given as a function of the two-jet invariant mass, M_{jj}. The faster increase of the gluon jet multiplicity is compensated by the reduced rate of gluon jets with increased M_{jj}. With the quark-gluon mixture of the model, good agreement with the data is obtained, taking the systematic error (± 1 particle both in data and model) of the extrapolation method in account. Extrapolation of the TASSO [23] quark jet multiplicities to collider energies (not explicitly shown) gives a reasonable agreement, within this sys-

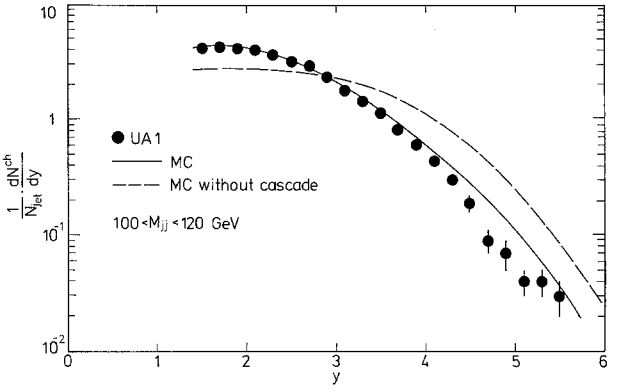

Fig. 3. Rapidity distribution of charged particles along the jet axis. UA1 data for jet-jet masses $100<M_{jj}<120$ GeV compared to model with (full curve) and without (dashed curve) parton cascade evolution

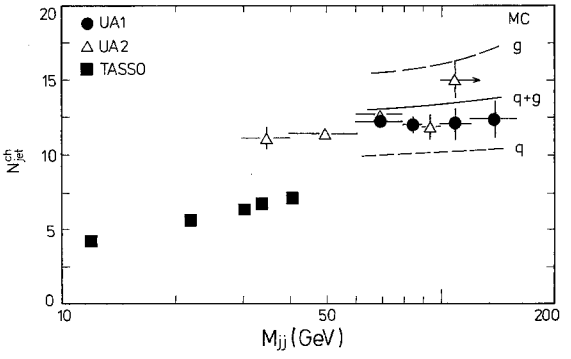

Fig. 4. Charged particle multiplicity, $N_{\rm jet}^{\rm ch}$ as defined in the text, of jets in a jet-jet system of mass M_{jj}. Data from UA1 [4], UA2 [2] and TASSO [23] compared with model results for quark and gluon jets separately as well as their proper mixture

tematic error, although a tendency for lower energy collider jets to have a larger multiplicity than expected from such an extrapolation can be observed. This may be related to the underlying event at the collider.

By integrating the distribution $z \cdot D(z)$, the fraction of the jet momentum carried by charged particles was found to be $\langle p_\parallel^{ch}/p_{jet}\rangle = 0.47 \pm 0.02 \pm 0.05$ in the UA1 data [4]. A similar value, 0.5, was found by AFS [3]. Given the size of the errors, the large event-by-event fluctuations of the charged energy fraction and the $z \to 0$ extrapolation, we do not consider this result significantly different from the Monte Carlo result of 0.61. Although this ratio varies with z, the small z-cut used (eq. (3)) implies a negligible bias.

Turning now to the transverse fragmentation properties within a jet, we show the inclusive $p_\perp$ distribution of charged particles, Fig. 5, and the variation of the mean $p_\perp$ along the jet, i.e. $\langle p_\perp\rangle(z)$ in Fig. 6. The jet axis is here defined by the momentum sum of all charged particles in the jet rather than by the calorimeter to avoid systematically overestimated relative $p_\perp$. In fact, the Monte Carlo result depends more on the details of the jet sample selection and the jet axis definition than on the model parameters, like t_{cut}. The rejection of three-jet events does, e.g., significantly reduce the rate of high-$p_\perp$ particles and thereby

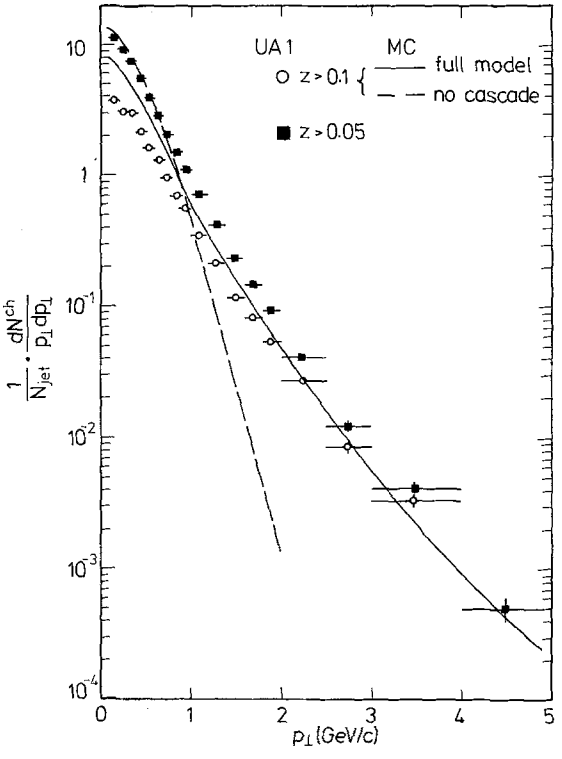

Fig. 5. Transverse momentum distribution of charged particles with respect to the jet axis. UA1 [4] data and model curves representing the inclusion (full curve) and omission (dashed curve) of gluon bremsstrahlung effects

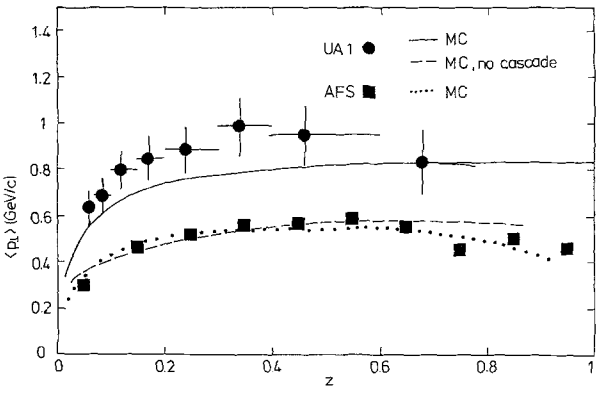

Fig. 6. Mean transverse momentum of charged particles with respect to the jet axis. UA1 [4] and AFS [3] data compared to the model. Full (dashed) curve is with (without) parton cascade at collider energies. Dotter curve is for ISR jets including parton cascade

decrease the $\langle p_\perp\rangle$. The low-$p_\perp$ part of the distribution in Fig. 5 depends sensitively on the cut applied to remove soft particles from the underlying event as illustrated with the two z-cuts shown for the data. Therefore, a small mismatch between data and model for the effective z-cut used may cause the observed difference at low $p_\perp$. Due to the exponential fall-off with $p_\perp$ the low $p_\perp$ region is important for the mean value, thus $\langle p_\perp\rangle = 730$ and 850 MeV/c in the data for $z > 0.05$ and 0.1 respectively. The slightly underestimated $\langle p_\perp\rangle$ of the model, Fig. 6, is thus partly related to its excess of low-$p_\perp$ particles in Fig. 5 and partly to the jet axis definition as mentioned. For the large-$p_\perp$ region the z-cut is of no importance. Here, however, the strong effect from the gluon radiation, as treated in the parton cascade, is clearly seen by comparing with the result obtained without it (dashed curve in Figs. 5 and 6). The ability of the QCD cascade model to describe the $p_\perp$-spectrum and the increase of $\langle p_\perp\rangle$ from ISR to the collider energies lends strong support to it.

4.2 Quark and Gluon Jet Results

A method to assign a flavour to each observed jet was devised in [4, 21]. From the measured two-jet kinematics, incoming parton momenta (x_1, x_2) and hard scattering variables $(\hat{s}, \hat{t}, \hat{u})$ are calculated and the subprocess cross-section

$$d\sigma_{ab\to cd} = f_a(x_1, Q^2) \cdot f_b(x_2, Q^2) \cdot \frac{d\hat{\sigma}}{d\hat{t}} dx_1\, dx_2\, d\hat{t} \qquad (5)$$

used to define the probability for a particular subprocess

$$P(ab \to cd) = \frac{d\sigma_{ab\to cd}}{\sum_{ijkl} d\sigma_{ij\to kl}} \qquad (6)$$

where the summation is over all $2 \to 2$ processes. The probability for a jet to be a gluon is then defined by

$$P_g = \sum_{a,b,X} P(ab \to \text{gluon} + X) \tag{7}$$

and $P_q = 1 - P_g$ is the probability that it is a quark jet. Jets with $P_g \geqq 0.55$ define a gluon enriched sample and those with $P_g \leqq 0.35$ a quark enriched sample. A further requirement of $|\cos\theta^*| \geqq 0.25$, where θ^* is the scattering angle in the parton c.m.s., was imposed to avoid ambigous configurations. In order to take the finite probabilities into account and estimate the pure quark and gluon distributions, a system of linear equations (see [4, 21] for details) was solved, for each z-bin, to obtain the experimental quark and gluon jet fragmentation functions in Fig. 7. (Note the restriction $z < 0.5$ in this figure, due to large statistical uncertainties for larger z-values).

In order to separate the quark-gluon differences from scaling violation effects, the Q^2-range is here restricted to $1{,}600 < Q^2 < 2{,}600\ \text{GeV}^2$. The gluon jets are, as expected, observed to be softer than the quark jets although the difference is not quite as pronounced as in the model calculation. A possible reason for this discrepancy could be the global jet energy correction applied to the data. If gluon jets are indeed softer than quark jets, their energy correction should be larger. An energy correction proportional to the gluon jet probability gives indeed a tendency for a larger difference, but this systematic uncertainty was estimated to be smaller than the statistical errors and was therefore not used [21]. If gluon jets, as expected, are wider than quark jets they will loose more energy outside the $\Delta R = 1$ cone. In the Monte Carlo events a typical energy loss is thus 12% for gluon jets and 8% for quark jets, but with a longer tail to larger energy losses for the gluon jets. Using a weighted mean value for the energy correction will thus tend to underestimate (overestimate) the gluon (quark) jet energy and thereby tend to produce a too hard (soft) gluon (quark) fragmentation function and thus reduce their difference.

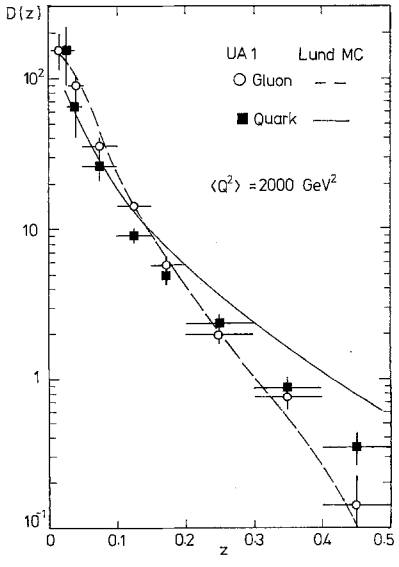

Fig. 7. Fragmentation function for quark and gluon jets, extracted as discussed in the text, from UA1 [4] data compared to model predictions for pure jet samples. (Note the restricted range of the z-variable).

Another possible difference between quark and gluon jets is their content of neutral and charged particles and the resulting electromagnetic and hadronic energies to which the calorimeter respond differently. Although the global charged energy fraction is found to be the same for quark and gluon jets in the data [4], it may be different for high energy particles. Within our model a gluon jet does indeed have relatively more high energy neutral particles, essentially π^0's giving photons to be absorbed in the electromagnetic calorimeter, as compared to a quark jet. A calorimeter 'e/π'-ratio larger than unity which is not fully corrected for will thus lead to a systematic difference of the measured energy of quark and gluon jets. If however gluons hadronize as a $q\bar{q}$ pair or a quark of random flavour, like assumed in ISAJET used for the energy correction estimate, this difference will not be present.

On the theoretical side there is the uncertainty that quark and gluon jet production cross-sections may have different higher order corrections which are not taken into account in the jet flavour assignement and which would affect the purity of the quark and gluon samples. Given the possible differences between quark and gluon jets just mentioned, it would be desirable to make energy corrections for quark and gluon jets separately. From the above discussion it is also clear, however, that this is extremely difficult to do in a model-independent way. The procedure of global energy corrections chosen for the data has only little model dependence. It need not, however, give the proper results for quark and gluon jets separately; a reduced quark-gluon difference may result as indicated.

The expected larger width of a gluon jet relative to a quark jet is shown in Fig. 8 in terms of the particle flow in the $\eta - \phi$ space, i.e. ΔR, relative to the calorimetric jet axis. Again the quark-gluon difference is slightly larger in the model. Given the uncertainties discussed above, we do not consider these differences between model and data to be significant enough to provide a real discrepancy.

Extending the method for jet flavour assignement

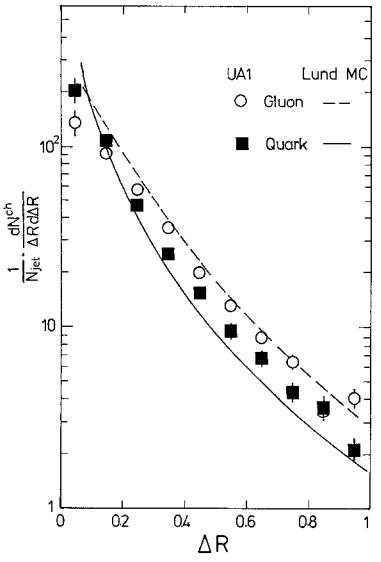

Fig. 8. Particle flow relative to jet axis, measured by ΔR in $\eta-\phi$ space, for purified quark and gluon jet samples of UA1 data and Monte Carlo model

Table 1. Charges for flavour assigned jets[a]

Jet flavour	$\langle Q_{jet}\rangle$ data	$\langle Q_{jet}\rangle$ Monte Carlo
gluon	-0.03 ± 0.01	0.0
u-quark	$+0.15\pm0.03$	$+0.19$
$\bar{u}$-quark	-0.15 ± 0.03	-0.19

[a] For the data, the jet flavour is defined by requiring that the corresponding probability is larger that 0.5, e.g. $P_g \geqq 0.5$, whereas the Monte Carlo results are obtained from a mixture of the known parton flavours to obtain the same probability. For the data an additional systematic error of approximately ± 0.02 should be added

in an obvious way to include also individual quark flavours it becomes interesting to relate the parton charges to the observed jet charges, defined by $Q_{jet} = \sum_i Q_i \cdot z_i^{1/3}$ with summation over all tracks in the jet. The results, shown in Table 1, agrees with the expectations from the model.

4.3 Scaling Violation Effects

To study scaling violation effects the data sample was divided into a low and high Q^2 region, $1{,}000 < Q^2 < 1{,}600$ and $2{,}600 < Q^2 < 4{,}000\ \mathrm{GeV}^2$ respectively. In order to avoid a varying quark-gluon mixture, which could introduce other variations than those due to the change of momentum transfer scale, this mixture was kept essentially fixed by selecting a gluon enriched sample with $P_g > 0.5$. A corresponding quark enriched sample suffers from limited statistics and was therefore not used. For the Monte Carlo result, pure quark and gluon jet results were mixed to obtain the same mean gluon probability of $\langle P_g \rangle = 0.65$ as in the data sample. The value of Q^2 is in both cases calculated from the 'measured" two-jet kinematics using the definition $Q^2 = \frac{2\hat{s}\hat{t}\hat{u}}{\hat{s}^2+\hat{t}^2+\hat{u}^2}$.

The resulting Q^2-dependence is shown in Fig. 9 for both the longitudinal and transverse jet properties. The variation of the data is in the direction anticipated, i.e. softer and wider jets at larger Q^2. The variation seem, however, to be slightly larger than that of the model. We note that, from the theoretical point of

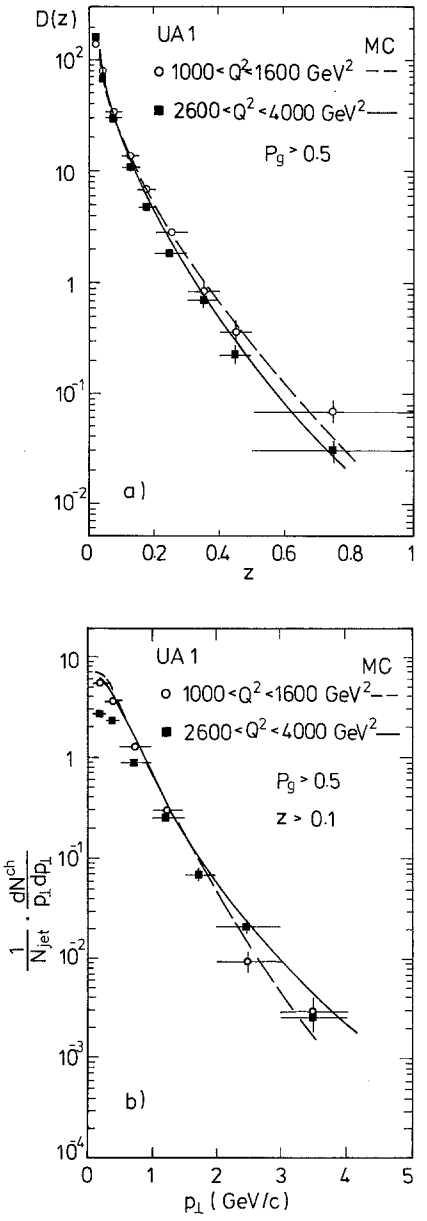

Fig. 9a, b. Fragmentation function **a** and charged particle $p_\perp$ relative to jet axis **b** for gluon enriched jet sample at two Q^2 scales showing scaling violations in UA1 data and Monte Carlo model

view, only small effects are anticipated since they scale with lnQ^2 only. In order to verify that the model results shown are not sensitive to parameters in the calculation, we have varied Λ_{QCD} and t_{cut} within reasonable limits and found the same magnitude of the Q^2 variation. Also a change of the offshellness scale, and its relation to the hard scattering variables, Q^2 and parton-parton invariant mass $\hat{s}$, does not lead to a significantly stronger Q^2 dependence. Furthermore, a simple cross check with another parton cascade evolution implementation [15] gives essentially the same result and we therefore conclude that the model result shown is very stable against variations of the theoretical framework.

We note that more important variations occur through changes of the relative quark-gluon mixture in the two samples. The gluon probability distribution is, however, essentially the same for the two data samples. To obtain an increased Q^2 dependence, the relative rate of gluon jets would have to increase with Q^2 contrary to normal expectations, unless higher order corrections (K-factors) invalidate this. We thus conclude that the Q^2 dependences expected from the QCD evolution is borne out by the data, which show a tendency to be somewhat stronger than anticipated although the precision of the data is not high enough for a firm conclusion on this point.

5. Discussion

The SPS collider jets studied here are produced at an energy scale which is an order of magnitude larger than previously available and therefore provides a challenge and interesting testing ground for current models for jet evolution and fragmentation. We have thus carried out a first detailed study by comparing data with theoretical expectations based on an elaborate Monte Carlo model. Globally, the jet properties are as expected and can be satisfactorily described by the model. By comparison with lower energy jets, e.g. at the ISR, we demonstrate the importance of the scaling violation effects originating from the radiation processes at the parton level. The parton cascade approximation based on QCD in the leading logarithm approach is able to describe this feature quite well when combined with a realistic model for the subsequent soft hadronization process. Comparisons of Monte Carlo results with analytic QCD calculations [24] give additional support for the implementation of the parton cascade approach presented here.

The main parameter, t_{cut}, which sets the mass-scale of the boundary between the perturbative and non-perturbative evolution of the parton jet to the final hadrons was here chosen as $\sqrt{t_{cut}}=4$ GeV, although a smaller value is acceptable by the UA1 data. The larger value used is only forced by the fragmentation function at large z observed for (quark) jets at the ISR. If this indication that non-perturbative effects set in at a mass scale of several GeV is verified by further studies, it would be important for our understanding of the hadronization mechanism. A consequence from such a scenario regarding heavy quark production in jets has been discussed in [25].

We have verified that the model results shown in this paper do not depend sensitively on the parameters of the model, which is in fact rather stable to such parameter variations within realistic limits. A particularly interesting variation of the model is the use of a conventional model for the parton cascade evolution [26], without the angular ordering prescription of [15] and therefore without taking soft gluon interference effects into account. We found no significant deviations compared to the coherent cascade and therefore conclude that, for the observables under investigation, the soft gluon interference do not produce observable effects. In [27] it has also been argued that the effects from the coherence are too small to be observable and well within the uncertainty associated with the parton cascade cutoff.

The SPS collider also provides the first opportunity to study gluon jets at an energy where they are clearly separable from the remaining event. This is particularly interesting since it has not been possible so far to make detailed comparisons of gluon jet fragmentation models with data and they are therefore poorely understood as compared to quark jets. We have studied separate quark and gluon jet samples and found systematic differences in the way expected from models, although the data show slightly smaller quark-gluon differences than the model. These deviations could, however, follow from a non-complete quark-gluon separation of the data sample and/or a slightly underestimated difference in the energy correction procedure as discussed above. These differences may also indicate an inadequacy of the particular model used and we note that other gluon fragmentation models can certainly be conceived of. One possibility [28], which can be included in the string model framework, is that a gluon stretches a colour octet field instead of two triplet fields as assumed in the Lund model [17]. The fragmentation properties of such an octet field are, however, not known so that modelling it would need new assumptions and parameters. One may expect that it breaks by gluon pair production (rather than $q\bar{q}$ production) leading to glueballs and SU(3) singlets [29] resulting in more leading neutral particles in gluon jets as compared to quark jets. The idea of preconfinement leading to intermediate mass colour singlet clusters is another

possibility [30, 31]. It is, however, beyond the scope of the present paper to make a detailed comparison also with these models, in particular since they are not so well developed for high-$p_\perp$ physics.

The data also show a tendency for a somewhat larger Q^2-evolution of the jet properties than expected from the model. However, both these deviations are small and the precision of the data not high enough to really make a clear discrepancy with respect to the model. The high-$p_\perp$ jets in hadronic interactions can thus be described relatively well using perturbative QCD and soft fragmentation based on e^+e^- data via the assumption of jet universality. We have in this study only considered the high-$p_\perp$ jets in a hadronic collision and neglected the underlying event with its spectator jets from the beam particle remnants. That part of the events is still poorely understood and provides a further challenge for model builders and Monte Carlo event generators.

Acknowledgements. We are grateful to T. Åkesson and T. Sjöstrand as well as members of the UA1 collaboration, in particular M. Della Negra, for interesting and helpful discussions.

References

1. UA2 Collab. P. Bagnaia et al.: Z. Phys. C – Particles and Fields **20**, 117 (1983); Phys. Lett. **138B**, 430 (1984); Phys. Lett. **144B**, 283 (1984); UA1 Collab. UA1 G. Arnison et al.: Phys. Lett. **132B**, 214 (1983); Phys. Lett. **136B**, 294 (1984)
2. UA2 Collab. P. Bagnaia et al.: Phys. Lett. **144B**, 291 (1984)
3. AFS Collab. T. Åkesson et al.: Z. Phys. C – Particles and Fields **30**, 27 (1986)
4. UA1 Collab. G. Arnison et al.: Nucl. Phys. **B276**, 253 (1986)
5. H.U. Bengtsson, G. Ingelman, T. Sjöstrand: The Lund Monte Carlo for high-$p_\perp$ scattering PYTHIA version 4.1
6. T. Sjöstrand: Comput. Phys. Commun. **39**, 347 (1986)
7. F.E. Paige, S.D. Protopopescu: Supercollider physics p. 41. Proceedings of the 1985 Oregon workshop on super high energy physics, Ed. D.E. Soper. Singapore: World Scientific
8. R. Odorico: Comput. Phys. Commun. **32**, 139 (1984)
9. R.D. Field, in: 1984 Summer study on the design and utilization of the Superconducting Super Collider (Snowmass, CO, 1984) p. 713 and UFTP-85-13
10. T.D. Gottschalk, Supercollider physics p. 3. Proceedings of the 1985 Oregon workshop on super high energy physics, Ed. D.E. Soper. Singapore: World Scientific
11. A. Ali, E. Pietarinen, B. van Eijk, to be published. B. van Eijk: Proceedings of 5th topical workshop on proton-antiproton collider physics, p. 165. Saint-Vincent, Italy, 1985, Ed. M. Greco. Singapore: World Scientific
12. T.D. Gottschalk: Supercollider Physics, p. 94. Proceedings of the 1985 Oregon workshop on super high energy physics, Ed. D.E. Soper. Singapore: World Scientific. F. Paige: p. 481 in proceedings of the 1985 international europhysics conference on high-energy physics, Bari, Italy; Ed. L. Nitti, G. Preparata, European Physical Society
13. E. Eichten, I. Hinchliffe, K. Lane, C. Quigg: Rev. Mod. Phys. **56**, 579 (1984)
14. G.C. Fox, S. Wolfram: Nucl. Phys. **B168**, 285 (1980); R.D. Field, S. Wolfram: Nucl. Phys. **B213**, 65 (1983); T.D. Gottschalk: Nucl. Phys. **B214-201**, (1983); CALT-68-1083 R. Odorico: Nucl. Phys. **B228**, 381 (1983)
15. G. Marchesini, B.R. Webber: Nucl. Phys. **B238**, 1 (1984); B.R. Webber: Nucl. Phys. **B238**, 492 (1984)
16. G. Ingelman: Phys. Scr. **33**, 39 (1986)
17. B. Andersson, G. Gustafson, G. Ingelman, T. Sjöstrand: Phys. Rep. **97**, 31 (1983)
18. T. Sjöstrand: Nucl. Phys. **B248**, 469 (1984)
19. T. Sjöstrand: Phys. Lett. **142B**, 420 (1984)
20. T. Sjöstrand: Phys. Lett. **157B**, 321 (1985)
21. P. Ghez: These d'Etat, LAPP-EXP/86-02
22. HRS Collab. M. Derrick et al.: Phys. Lett. **164B**, 199 (1985)
23. TASSO Colab. M. Althoff et al.: Z. Phys. C – Particles and Fields **22**, 307 (1984)
24. G. Ingelman, D.E. Soper: Phys. Lett. **148B**, 171 (1984)
25. A. Ali, G. Ingelman: Phys. Lett. **156B**, 111 (1985)
26. We used the conventional cascade implemented in [6] which is based on K. Kajantie, E. Pietarinen: Phys. Lett. **93B**, 269 (1980)
27. R. Odorico: Z. Phys. C – Particles and Fields **30**, 257 (1986)
28. I. Montvay: Phys. Lett. **84B**, 331 (1979)
29. C. Peterson, T.F. Walsh: Phys. Lett. **91B**, 455 (1980)
30. D. Amati, G. Veneziano: Phys. Lett. **83B**, 87 (1979)
31. C.-K. Ng: Phys. Rev. **D31**, 469 (1985)